BABAR-CONF-05/14
SLAC-PUB-11368
hep-ex/0507087
July 2005

Measurement of Time-Dependent *CP*-Violating Asymmetries in B^0 Meson Decays to $\eta' K^0_L$

The *BABAR* Collaboration

August 19, 2005

Abstract

We present a preliminary measurement of *CP*-violating parameters S and C from fits of the time-dependence of B^0 meson decays to $\eta' K^0_L$. The data were recorded with the *BABAR* detector at PEP-II and correspond to 232×10^6 $B\overline{B}$ pairs produced in e^+e^- annihilation through the $\Upsilon(4S)$ resonance. By fitting the time-dependent *CP* asymmetry of the reconstructed $B^0 \to \eta' K^0_L$ events, we find $S = 0.60 \pm 0.31 \pm 0.04$ and $C = 0.10 \pm 0.21 \pm 0.03$, where the first error quoted is statistical and the second is systematic. We also perform a combined fit using both $\eta' K^0_S$ and $\eta' K^0_L$ data, and find $S = 0.36 \pm 0.13 \pm 0.03$ and $C = -0.16 \pm 0.09 \pm 0.02$.

Submitted at the International Europhysics Conference On High-Energy Physics (HEP 2005), 7/21—7/27/2005, Lisbon, Portugal

Stanford Linear Accelerator Center, Stanford University, Stanford, CA 94309

Work supported in part by Department of Energy contract DE-AC02-76SF00515.

The *BABAR* Collaboration,

B. Aubert, R. Barate, D. Boutigny, F. Couderc, Y. Karyotakis, J. P. Lees, V. Poireau, V. Tisserand, A. Zghiche

Laboratoire de Physique des Particules, F-74941 Annecy-le-Vieux, France

E. Grauges

IFAE, Universitat Autonoma de Barcelona, E-08193 Bellaterra, Barcelona, Spain

A. Palano, M. Pappagallo, A. Pompili

Università di Bari, Dipartimento di Fisica and INFN, I-70126 Bari, Italy

J. C. Chen, N. D. Qi, G. Rong, P. Wang, Y. S. Zhu

Institute of High Energy Physics, Beijing 100039, China

G. Eigen, I. Ofte, B. Stugu

University of Bergen, Institute of Physics, N-5007 Bergen, Norway

G. S. Abrams, M. Battaglia, A. B. Breon, D. N. Brown, J. Button-Shafer, R. N. Cahn, E. Charles, C. T. Day, M. S. Gill, A. V. Gritsan, Y. Groysman, R. G. Jacobsen, R. W. Kadel, J. Kadyk, L. T. Kerth, Yu. G. Kolomensky, G. Kukartsev, G. Lynch, L. M. Mir, P. J. Oddone, T. J. Orimoto, M. Pripstein, N. A. Roe, M. T. Ronan, W. A. Wenzel

Lawrence Berkeley National Laboratory and University of California, Berkeley, California 94720, USA

M. Barrett, K. E. Ford, T. J. Harrison, A. J. Hart, C. M. Hawkes, S. E. Morgan, A. T. Watson

University of Birmingham, Birmingham, B15 2TT, United Kingdom

M. Fritsch, K. Goetzen, T. Held, H. Koch, B. Lewandowski, M. Pelizaeus, K. Peters, T. Schroeder, M. Steinke

Ruhr Universität Bochum, Institut für Experimentalphysik 1, D-44780 Bochum, Germany

J. T. Boyd, J. P. Burke, N. Chevalier, W. N. Cottingham

University of Bristol, Bristol BS8 1TL, United Kingdom

T. Cuhadar-Donszelmann, B. G. Fulsom, C. Hearty, N. S. Knecht, T. S. Mattison, J. A. McKenna

University of British Columbia, Vancouver, British Columbia, Canada V6T 1Z1

A. Khan, P. Kyberd, M. Saleem, L. Teodorescu

Brunel University, Uxbridge, Middlesex UB8 3PH, United Kingdom

A. E. Blinov, V. E. Blinov, A. D. Bukin, V. P. Druzhinin, V. B. Golubev, E. A. Kravchenko, A. P. Onuchin, S. I. Serednyakov, Yu. I. Skovpen, E. P. Solodov, A. N. Yushkov

Budker Institute of Nuclear Physics, Novosibirsk 630090, Russia

D. Best, M. Bondioli, M. Bruinsma, M. Chao, S. Curry, I. Eschrich, D. Kirkby, A. J. Lankford, P. Lund, M. Mandelkern, R. K. Mommsen, W. Roethel, D. P. Stoker

University of California at Irvine, Irvine, California 92697, USA

C. Buchanan, B. L. Hartfiel, A. J. R. Weinstein

University of California at Los Angeles, Los Angeles, California 90024, USA

S. D. Foulkes, J. W. Gary, O. Long, B. C. Shen, K. Wang, L. Zhang
University of California at Riverside, Riverside, California 92521, USA

D. del Re, H. K. Hadavand, E. J. Hill, D. B. MacFarlane, H. P. Paar, S. Rahatlou, V. Sharma
University of California at San Diego, La Jolla, California 92093, USA

J. W. Berryhill, C. Campagnari, A. Cunha, B. Dahmes, T. M. Hong, M. A. Mazur, J. D. Richman, W. Verkerke
University of California at Santa Barbara, Santa Barbara, California 93106, USA

T. W. Beck, A. M. Eisner, C. J. Flacco, C. A. Heusch, J. Kroseberg, W. S. Lockman, G. Nesom, T. Schalk, B. A. Schumm, A. Seiden, P. Spradlin, D. C. Williams, M. G. Wilson
University of California at Santa Cruz, Institute for Particle Physics, Santa Cruz, California 95064, USA

J. Albert, E. Chen, G. P. Dubois-Felsmann, A. Dvoretskii, D. G. Hitlin, I. Narsky, T. Piatenko, F. C. Porter, A. Ryd, A. Samuel
California Institute of Technology, Pasadena, California 91125, USA

R. Andreassen, S. Jayatilleke, G. Mancinelli, B. T. Meadows, M. D. Sokoloff
University of Cincinnati, Cincinnati, Ohio 45221, USA

F. Blanc, P. Bloom, S. Chen, W. T. Ford, J. F. Hirschauer, A. Kreisel, U. Nauenberg, A. Olivas, P. Rankin, W. O. Ruddick, J. G. Smith, K. A. Ulmer, S. R. Wagner, J. Zhang
University of Colorado, Boulder, Colorado 80309, USA

A. Chen, E. A. Eckhart, J. L. Harton, A. Soffer, W. H. Toki, R. J. Wilson, Q. Zeng
Colorado State University, Fort Collins, Colorado 80523, USA

D. Altenburg, E. Feltresi, A. Hauke, B. Spaan
Universität Dortmund, Institut fur Physik, D-44221 Dortmund, Germany

T. Brandt, J. Brose, M. Dickopp, V. Klose, H. M. Lacker, R. Nogowski, S. Otto, A. Petzold, G. Schott, J. Schubert, K. R. Schubert, R. Schwierz, J. E. Sundermann
Technische Universität Dresden, Institut für Kern- und Teilchenphysik, D-01062 Dresden, Germany

D. Bernard, G. R. Bonneaud, P. Grenier, S. Schrenk, Ch. Thiebaux, G. Vasileiadis, M. Verderi
Ecole Polytechnique, LLR, F-91128 Palaiseau, France

D. J. Bard, P. J. Clark, W. Gradl, F. Muheim, S. Playfer, Y. Xie
University of Edinburgh, Edinburgh EH9 3JZ, United Kingdom

M. Andreotti, V. Azzolini, D. Bettoni, C. Bozzi, R. Calabrese, G. Cibinetto, E. Luppi, M. Negrini, L. Piemontese
Università di Ferrara, Dipartimento di Fisica and INFN, I-44100 Ferrara, Italy

F. Anulli, R. Baldini-Ferroli, A. Calcaterra, R. de Sangro, G. Finocchiaro, P. Patteri, I. M. Peruzzi,[1] M. Piccolo, A. Zallo
Laboratori Nazionali di Frascati dell'INFN, I-00044 Frascati, Italy

[1]Also with Università di Perugia, Dipartimento di Fisica, Perugia, Italy

A. Buzzo, R. Capra, R. Contri, M. Lo Vetere, M. Macri, M. R. Monge, S. Passaggio, C. Patrignani, E. Robutti, A. Santroni, S. Tosi

Università di Genova, Dipartimento di Fisica and INFN, I-16146 Genova, Italy

G. Brandenburg, K. S. Chaisanguanthum, M. Morii, E. Won, J. Wu

Harvard University, Cambridge, Massachusetts 02138, USA

R. S. Dubitzky, U. Langenegger, J. Marks, S. Schenk, U. Uwer

Universität Heidelberg, Physikalisches Institut, Philosophenweg 12, D-69120 Heidelberg, Germany

W. Bhimji, D. A. Bowerman, P. D. Dauncey, U. Egede, R. L. Flack, J. R. Gaillard, G. W. Morton, J. A. Nash, M. B. Nikolich, G. P. Taylor, W. P. Vazquez

Imperial College London, London, SW7 2AZ, United Kingdom

M. J. Charles, W. F. Mader, U. Mallik, A. K. Mohapatra

University of Iowa, Iowa City, Iowa 52242, USA

J. Cochran, H. B. Crawley, V. Eyges, W. T. Meyer, S. Prell, E. I. Rosenberg, A. E. Rubin, J. Yi

Iowa State University, Ames, Iowa 50011-3160, USA

N. Arnaud, M. Davier, X. Giroux, G. Grosdidier, A. Höcker, F. Le Diberder, V. Lepeltier, A. M. Lutz, A. Oyanguren, T. C. Petersen, M. Pierini, S. Plaszczynski, S. Rodier, P. Roudeau, M. H. Schune, A. Stocchi, G. Wormser

Laboratoire de l'Accélérateur Linéaire, F-91898 Orsay, France

C. H. Cheng, D. J. Lange, M. C. Simani, D. M. Wright

Lawrence Livermore National Laboratory, Livermore, California 94550, USA

A. J. Bevan, C. A. Chavez, I. J. Forster, J. R. Fry, E. Gabathuler, R. Gamet, K. A. George, D. E. Hutchcroft, R. J. Parry, D. J. Payne, K. C. Schofield, C. Touramanis

University of Liverpool, Liverpool L69 72E, United Kingdom

C. M. Cormack, F. Di Lodovico, W. Menges, R. Sacco

Queen Mary, University of London, E1 4NS, United Kingdom

C. L. Brown, G. Cowan, H. U. Flaecher, M. G. Green, D. A. Hopkins, P. S. Jackson, T. R. McMahon, S. Ricciardi, F. Salvatore

University of London, Royal Holloway and Bedford New College, Egham, Surrey TW20 0EX, United Kingdom

D. Brown, C. L. Davis

University of Louisville, Louisville, Kentucky 40292, USA

J. Allison, N. R. Barlow, R. J. Barlow, C. L. Edgar, M. C. Hodgkinson, M. P. Kelly, G. D. Lafferty, M. T. Naisbit, J. C. Williams

University of Manchester, Manchester M13 9PL, United Kingdom

C. Chen, W. D. Hulsbergen, A. Jawahery, D. Kovalskyi, C. K. Lae, D. A. Roberts, G. Simi

University of Maryland, College Park, Maryland 20742, USA

G. Blaylock, C. Dallapiccola, S. S. Hertzbach, R. Kofler, V. B. Koptchev, X. Li, T. B. Moore, S. Saremi, H. Staengle, S. Willocq

University of Massachusetts, Amherst, Massachusetts 01003, USA

R. Cowan, K. Koeneke, G. Sciolla, S. J. Sekula, M. Spitznagel, F. Taylor, R. K. Yamamoto

Massachusetts Institute of Technology, Laboratory for Nuclear Science, Cambridge, Massachusetts 02139, USA

H. Kim, P. M. Patel, S. H. Robertson

McGill University, Montréal, Quebec, Canada H3A 2T8

A. Lazzaro, V. Lombardo, F. Palombo

Università di Milano, Dipartimento di Fisica and INFN, I-20133 Milano, Italy

J. M. Bauer, L. Cremaldi, V. Eschenburg, R. Godang, R. Kroeger, J. Reidy, D. A. Sanders, D. J. Summers, H. W. Zhao

University of Mississippi, University, Mississippi 38677, USA

S. Brunet, D. Côté, P. Taras, B. Viaud

Université de Montréal, Laboratoire René J. A. Lévesque, Montréal, Quebec, Canada H3C 3J7

H. Nicholson

Mount Holyoke College, South Hadley, Massachusetts 01075, USA

N. Cavallo,[2] G. De Nardo, F. Fabozzi,[2] C. Gatto, L. Lista, D. Monorchio, P. Paolucci, D. Piccolo, C. Sciacca

Università di Napoli Federico II, Dipartimento di Scienze Fisiche and INFN, I-80126, Napoli, Italy

M. Baak, H. Bulten, G. Raven, H. L. Snoek, L. Wilden

NIKHEF, National Institute for Nuclear Physics and High Energy Physics, NL-1009 DB Amsterdam, The Netherlands

C. P. Jessop, J. M. LoSecco

University of Notre Dame, Notre Dame, Indiana 46556, USA

T. Allmendinger, G. Benelli, K. K. Gan, K. Honscheid, D. Hufnagel, P. D. Jackson, H. Kagan, R. Kass, T. Pulliam, A. M. Rahimi, R. Ter-Antonyan, Q. K. Wong

Ohio State University, Columbus, Ohio 43210, USA

J. Brau, R. Frey, O. Igonkina, M. Lu, C. T. Potter, N. B. Sinev, D. Strom, J. Strube, E. Torrence

University of Oregon, Eugene, Oregon 97403, USA

F. Galeazzi, M. Margoni, M. Morandin, M. Posocco, M. Rotondo, F. Simonetto, R. Stroili, C. Voci

Università di Padova, Dipartimento di Fisica and INFN, I-35131 Padova, Italy

M. Benayoun, H. Briand, J. Chauveau, P. David, L. Del Buono, Ch. de la Vaissière, O. Hamon, M. J. J. John, Ph. Leruste, J. Malclès, J. Ocariz, L. Roos, G. Therin

Universités Paris VI et VII, Laboratoire de Physique Nucléaire et de Hautes Energies, F-75252 Paris, France

[2]Also with Università della Basilicata, Potenza, Italy

P. K. Behera, L. Gladney, Q. H. Guo, J. Panetta
University of Pennsylvania, Philadelphia, Pennsylvania 19104, USA

M. Biasini, R. Covarelli, S. Pacetti, M. Pioppi
Università di Perugia, Dipartimento di Fisica and INFN, I-06100 Perugia, Italy

C. Angelini, G. Batignani, S. Bettarini, F. Bucci, G. Calderini, M. Carpinelli, R. Cenci, F. Forti, M. A. Giorgi, A. Lusiani, G. Marchiori, M. Morganti, N. Neri, E. Paoloni, M. Rama, G. Rizzo, J. Walsh
Università di Pisa, Dipartimento di Fisica, Scuola Normale Superiore and INFN, I-56127 Pisa, Italy

M. Haire, D. Judd, D. E. Wagoner
Prairie View A&M University, Prairie View, Texas 77446, USA

J. Biesiada, N. Danielson, P. Elmer, Y. P. Lau, C. Lu, J. Olsen, A. J. S. Smith, A. V. Telnov
Princeton University, Princeton, New Jersey 08544, USA

F. Bellini, G. Cavoto, A. D'Orazio, E. Di Marco, R. Faccini, F. Ferrarotto, F. Ferroni, M. Gaspero, L. Li Gioi, M. A. Mazzoni, S. Morganti, G. Piredda, F. Polci, F. Safai Tehrani, C. Voena
Università di Roma La Sapienza, Dipartimento di Fisica and INFN, I-00185 Roma, Italy

H. Schröder, G. Wagner, R. Waldi
Universität Rostock, D-18051 Rostock, Germany

T. Adye, N. De Groot, B. Franek, G. P. Gopal, E. O. Olaiya, F. F. Wilson
Rutherford Appleton Laboratory, Chilton, Didcot, Oxon, OX11 0QX, United Kingdom

R. Aleksan, S. Emery, A. Gaidot, S. F. Ganzhur, P.-F. Giraud, G. Graziani, G. Hamel de Monchenault, W. Kozanecki, M. Legendre, G. W. London, B. Mayer, G. Vasseur, Ch. Yèche, M. Zito
DSM/Dapnia, CEA/Saclay, F-91191 Gif-sur-Yvette, France

M. V. Purohit, A. W. Weidemann, J. R. Wilson, F. X. Yumiceva
University of South Carolina, Columbia, South Carolina 29208, USA

T. Abe, M. T. Allen, D. Aston, N. van Bakel, R. Bartoldus, N. Berger, A. M. Boyarski, O. L. Buchmueller, R. Claus, J. P. Coleman, M. R. Convery, M. Cristinziani, J. C. Dingfelder, D. Dong, J. Dorfan, D. Dujmic, W. Dunwoodie, S. Fan, R. C. Field, T. Glanzman, S. J. Gowdy, T. Hadig, V. Halyo, C. Hast, T. Hryn'ova, W. R. Innes, M. H. Kelsey, P. Kim, M. L. Kocian, D. W. G. S. Leith, J. Libby, S. Luitz, V. Luth, H. L. Lynch, H. Marsiske, R. Messner, D. R. Muller, C. P. O'Grady, V. E. Ozcan, A. Perazzo, M. Perl, B. N. Ratcliff, A. Roodman, A. A. Salnikov, R. H. Schindler, J. Schwiening, A. Snyder, J. Stelzer, D. Su, M. K. Sullivan, K. Suzuki, S. Swain, J. M. Thompson, J. Va'vra, M. Weaver, W. J. Wisniewski, M. Wittgen, D. H. Wright, A. K. Yarritu, K. Yi, C. C. Young
Stanford Linear Accelerator Center, Stanford, California 94309, USA

P. R. Burchat, A. J. Edwards, S. A. Majewski, B. A. Petersen, C. Roat
Stanford University, Stanford, California 94305-4060, USA

M. Ahmed, S. Ahmed, M. S. Alam, J. A. Ernst, M. A. Saeed, F. R. Wappler, S. B. Zain
State University of New York, Albany, New York 12222, USA

W. Bugg, M. Krishnamurthy, S. M. Spanier
University of Tennessee, Knoxville, Tennessee 37996, USA

R. Eckmann, J. L. Ritchie, A. Satpathy, R. F. Schwitters
University of Texas at Austin, Austin, Texas 78712, USA

J. M. Izen, I. Kitayama, X. C. Lou, S. Ye
University of Texas at Dallas, Richardson, Texas 75083, USA

F. Bianchi, M. Bona, F. Gallo, D. Gamba
Università di Torino, Dipartimento di Fisica Sperimentale and INFN, I-10125 Torino, Italy

M. Bomben, L. Bosisio, C. Cartaro, F. Cossutti, G. Della Ricca, S. Dittongo, S. Grancagnolo, L. Lanceri, L. Vitale
Università di Trieste, Dipartimento di Fisica and INFN, I-34127 Trieste, Italy

F. Martinez-Vidal
IFIC, Universitat de Valencia-CSIC, E-46071 Valencia, Spain

R. S. Panvini[3]
Vanderbilt University, Nashville, Tennessee 37235, USA

Sw. Banerjee, B. Bhuyan, C. M. Brown, D. Fortin, K. Hamano, R. Kowalewski, J. M. Roney, R. J. Sobie
University of Victoria, Victoria, British Columbia, Canada V8W 3P6

J. J. Back, P. F. Harrison, T. E. Latham, G. B. Mohanty
Department of Physics, University of Warwick, Coventry CV4 7AL, United Kingdom

H. R. Band, X. Chen, B. Cheng, S. Dasu, M. Datta, A. M. Eichenbaum, K. T. Flood, M. Graham, J. J. Hollar, J. R. Johnson, P. E. Kutter, H. Li, R. Liu, B. Mellado, A. Mihalyi, Y. Pan, R. Prepost, P. Tan, J. H. von Wimmersperg-Toeller, S. L. Wu, Z. Yu
University of Wisconsin, Madison, Wisconsin 53706, USA

H. Neal
Yale University, New Haven, Connecticut 06511, USA

[3]Deceased

1 Introduction

Decays of B^0 mesons to charmless hadronic final states such as ϕK^0, $K^+K^-K^0$, $\eta' K^0$, $\pi^0 K^0$ and $f_0(980)K^0$ proceed mostly via a single penguin (loop) amplitude with the same weak phase as in B decays to a charmonium state plus a K^0 meson [1, 2]. However Cabibbo-Kobayashi-Maskawa (CKM)-suppressed amplitudes and new particles in the loop can introduce other weak phases whose contribution is not negligible [1, 3].

Fig. 1(a) shows the diagram describing the $B - \bar{B}$ mixing. The amplitudes shown in Fig. 1(b)-(d) are relevant for the decay $B^0 \to \eta' K^0$. All of the amplitudes are suppressed by small CKM matrix elements, but the tree diagram for B^0 shown in Fig. 1(d) is expected to be smaller [2, 4] since there is additional CKM suppression and color suppression.

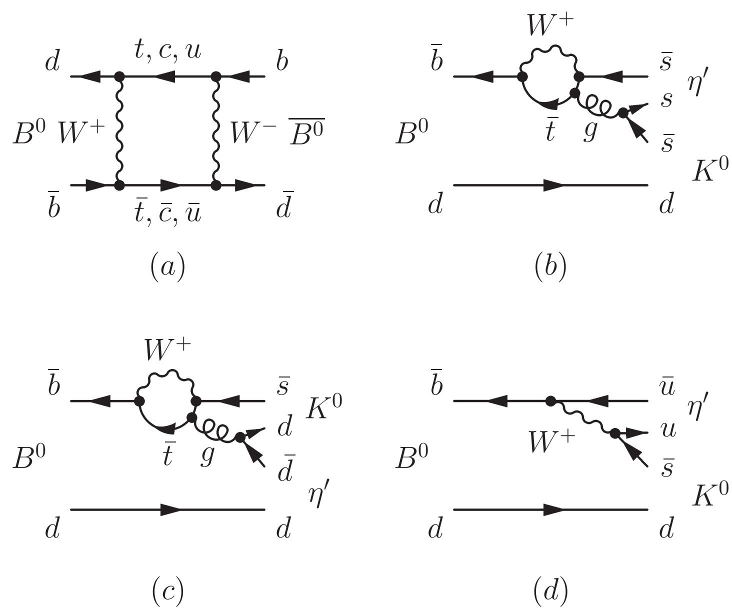

Figure 1: Feynman diagrams describing (a) $B - \bar{B}$ mixing, the decay $B^0 \to \eta' K^0$ via (b, c) internal gluonic penguin and (d) color-suppressed tree.

For the decay $B^0 \to \eta' K^0$, the additional contributions of other weak phases from CKM-suppressed amplitudes are expected to be small, so the time-dependent *CP* asymmetry measurement provides an approximate measurement of sin2β. We define S and C as the coefficients of sine and cosine oscillation terms, respectively, in the $B\bar{B}$ decay rate distributions (see Eqn. (1) below). ΔS is the deviation between S in the decay $B^0 \to \eta' K^0$ and S, equal to sin2β, in the charmonium K^0 decays. Theoretical bounds for this deviation have been calculated with an SU(3) analysis [5, 6]. Such bounds have been improved [7] by the measurements of B^0 decays to a pair of neutral charmless light pseudoscalar mesons [8, 9], with the conclusion that ΔS is expected to be less than 0.10 (with a theoretical uncertainty less than $\sim$0.03 due to the assumptions in the calculation). QCD factorization calculations conclude that ΔS is even smaller [10]. A significantly larger value of ΔS could arise from non-Standard-Model amplitudes [3].

The *CP*-violating asymmetry in the decay $B^0 \to \eta' K^0$ has been measured previously by the *BABAR* [11] and Belle [12] experiments using the final state $\eta' K^0_S$. In the measurement presented in this paper we use events reconstructed in the $\eta' K^0_L$ final state. We present also the measurement of *CP*-violating asymmetry combining present $\eta' K^0_L$ data with the $\eta' K^0_S$ data used in the previous *BABAR* measurement [11].

2 The *BABAR* Detector and Dataset

The results presented in this paper are based on data collected in 1999–2004 with the *BABAR* detector [13] at the PEP-II asymmetric e^+e^- collider [14] located at the Stanford Linear Accelerator Center. An integrated luminosity of 211 fb^{-1}, corresponding to about 232 million $B\overline{B}$ pairs, was recorded at the $\Upsilon(4S)$ resonance ("on-resonance", center-of-mass energy $\sqrt{s} = 10.58$ GeV).

The asymmetric beam configuration in the laboratory frame provides a boost of $\beta\gamma = 0.56$ to the $\Upsilon(4S)$. Charged particles are detected and their momenta measured by the combination of a silicon vertex tracker (SVT), consisting of five layers of double-sided detectors, and a 40-layer central drift chamber, both operating in the 1.5 T magnetic field of a solenoid. The tracking system covers 92% of the solid angle in the center-of-mass (CM) frame.

Charged-particle identification (PID) is provided by the average energy loss ($\mathrm{d}E/\mathrm{d}x$) in the tracking devices and by an internally reflecting ring-imaging Cherenkov detector (DIRC) covering the central region. A K/π separation of better than four standard deviations (σ) is achieved for momenta below 3 GeV/c, decreasing to 2.5 σ at the highest momenta in the B decay final states. Photons and electrons are detected by a CsI(Tl) electromagnetic calorimeter (EMC). The EMC provides good energy and angular resolutions for detection of photons in the range from 30 MeV to 4 GeV. The energy and angular resolutions are 3% and 4 mrad, respectively, for a 1 GeV photon.

The flux return (IFR) for the solenoid is composed of multiple layers of iron and resistive plate chambers for the identification of muons and long-lived neutral hadrons.

3 Event Selection and Analysis Method

Monte Carlo (MC) simulations of the signal decay modes, $B\overline{B}$ backgrounds, and detector response are used to establish the event selection criteria. We reconstruct η' mesons through the decays $\eta' \to \rho^0\gamma$ ($\eta'_{\rho\gamma}$) and $\eta' \to \eta\pi^+\pi^-$ ($\eta'_{\eta\pi\pi}$) with $\eta \to \gamma\gamma$. The photon energy E_γ in laboratory system must be greater than 50 MeV for η candidates, and greater than 200 MeV in $\eta'_{\rho\gamma}$. We make the following requirements on the invariant masses (in MeV/c^2): $490 < m_{\gamma\gamma} < 600$ for η, $510 < m_{\pi\pi} < 1000$ for ρ^0, $945 < m_{\eta\pi\pi} < 970$ for $\eta'_{\eta\pi\pi}$, and $930 < m_{\rho\gamma} < 980$ for $\eta'_{\rho\gamma}$. We require the PID information of the signal pions to be consistent with the pion hypothesis.

Signal K^0_L candidates are reconstructed from clusters of energy deposited in the EMC or from hits in the IFR not associated to any charged track in the event. Because the energy of the K^0_L is not measured, we determine the K^0_L candidate laboratory momentum from its flight direction determined from the η' vertex and the centroid of the EMC (or IFR) candidate and the constraints of K^0_L and B^0 masses to their nominal values [15].

A B meson candidate is characterized kinematically by the energy difference $\Delta E \equiv E^*_B - \frac{1}{2}\sqrt{s}$, where E^*_B is the CM energy of the B meson. Signal events are peaked within ± 10 MeV of $\Delta E = 0$ while background events extend towards positive values of ΔE (this is a consequence of the mass constraint used to determine the K^0_L momentum). We require $-0.01 < \Delta E < 0.08$ GeV. This choice is dictated by the need of preserving a region with enough background for a fit to that component.

To reject background due to continuum $e^+e^- \to q\overline{q}$ events ($q = u, d, s, c$), we make use of the angle θ_T between the thrust axis of the B candidate and that of the rest of the tracks and neutral clusters in the event, calculated in the center-of-mass frame. The distribution of $\cos\theta_T$ is sharply peaked near ± 1 for combinations drawn from jet-like $q\bar{q}$ pairs and is nearly uniform for the isotropic B meson decays; we require $|\cos\theta_T| < 0.8$ in the $\eta' \to \eta\pi^+\pi^-$ subdecay mode and $|\cos\theta_T| < 0.75$ in the $\eta' \to \rho^0\gamma$ subdecay.

For further suppression of continuum background we require that the total missing transverse momentum projected along the K_L^0 direction, where the total momentum is calculated with all charged tracks and neutral clusters (without the K_L^0), is no more than 0.45 GeV/c lower than the calculated transverse momentum of the K_L^0 candidate. We also require that the cosine of the polar angle θ of the total missing momentum in laboratory system to be less than 0.95.

The purity of the K_L^0 candidates reconstructed in the EMC is further improved by a cut on the output of a neural network (NN) that takes cluster-shape variables as its inputs. The NN was trained using MC signal events and data events in the side band distribution (defined as $0.04 < \Delta E < 0.08$ GeV). We validated the performance of the NN using K_L^0 candidates in the reconstructed $B^0 \to J/\psi K_L^0$ events.

All selection criteria have been chosen using MC signal and background events to maximize the expected statistical significance of signal yield in the data.

The $B\overline{B}$ backgrounds were estimated using Monte Carlo simulations of $B^0\overline{B}^0$ and B^+B^-. We found a small evidence of $B\overline{B}$ background from $b \to c$ decays in the sub-decay mode $\eta' \to \rho^0\gamma$, so we added this component to the fit.

For each $B^0 \to \eta' K_L^0$ candidate (B_{CP}), we reconstruct the decay vertex of the other B meson ($B_{\rm tag}$) from the remaining charged tracks in the event and identify its flavor. The time difference $\Delta t \equiv t_{CP} - t_{\rm tag}$, where t_{CP} and $t_{\rm tag}$ are the proper decay times of the B_{CP} and $B_{\rm tag}$, respectively, is obtained from the measured distance between the B_{CP} and $B_{\rm tag}$ decay vertices and from the boost ($\beta\gamma = 0.56$) of the e^+e^- beam system. The distribution of Δt is:

$$F(\Delta t) = \frac{e^{-|\Delta t|/\tau}}{4\tau} \left\{1 \mp \Delta\omega \pm (1-2\omega)\left[-\eta S \sin(\Delta m_d \Delta t) - C\cos(\Delta m_d \Delta t)\right]\right\}, \tag{1}$$

where the upper (lower) sign denotes a decay accompanied by a B^0 ($\overline{B}^0$) tag, τ is the mean B^0 lifetime, Δm_d is the mixing frequency, η is the CP eigenvalue of the final state ($\eta = +1$ for $\eta' K_L^0$, $\eta = -1$ for $\eta' K_S^0$) and the mistag parameters ω and $\Delta\omega$ are the average and difference, respectively, of the probabilities that a true B^0 ($\overline{B}^0$) meson is tagged as $\overline{B}^0$ (B^0). The tagging algorithm, based on six tagging categories, is an improved version of what was used in the previous *BABAR* publication [11]. Separate neural networks are trained to identify primary leptons, kaons, soft pions from D^* decays, and high-momentum charged particles from B decays. Each event is assigned to one of the tagging categories based on the source of tagging information and on the estimated mistag probability. The distribution $F(\Delta t)$ is convolved with a resolution function to account for the finite vertex resolution of the detector.

4 Maximum Likelihood Fit

We use an unbinned, multivariate maximum-likelihood fit to extract signal yields and CP violating parameters. We use the following discriminating variables: ΔE, a Fisher discriminant $\mathcal{F}$, Δt. In the decay mode $\eta' \to \rho^0\gamma$ we add the η' mass and the variable $\mathcal{H}$, defined as the cosine of the ρ meson's rest frame decay angle of a pion with respect to the η' flight direction. The Fisher discriminant combines four variables: the angles with respect to the beam axis of the B momentum and B thrust axis in the $\Upsilon(4S)$ frame, and the zeroth and second angular moments of the energy flow excluding the B candidate around the B thrust axis.

We indicate with j the event species: signal, continuum background, or $B\overline{B}$ background. For each species j and each flavor-tagging category c, we define a total probability density function (PDF) for an events i as:

$$\mathcal{P}^i_{j,c} = \mathcal{P}_j(\Delta E^i)\,\mathcal{P}_j(\mathcal{F}^i)\,\mathcal{P}_j(M^i_{\eta'})\,\mathcal{P}_j(\mathcal{H}^i)\,\mathcal{P}_j(\Delta t^i, \sigma^i_{\Delta t}, c). \tag{2}$$

where $\sigma^i_{\Delta t}$ is the error on Δt for an event i. We define the extended likelihood function for the N_c input events in category c as

$$\mathcal{L}_c = \exp\left(-\sum_j n_j f_{j,c}\right)\prod_i^{N_c}(n_{\rm sig}f_{{\rm sig},c}\mathcal{P}^i_{{\rm sig},c} + n_{q\bar{q}}f_{q\bar{q},c}\mathcal{P}^i_{q\bar{q}} + n_{B\bar{B}}f_{B\bar{B},c}\mathcal{P}^i_{B\bar{B}}), \tag{3}$$

where n_j is the number of events with species j, and $f_{j,c}$ is the fraction of category-c events with species j. We fix $f_{sig,c}$ and $f_{B\bar{B},c}$ to $f_{B_{flav},c}$, the values measured with a sample of neutral B decays to flavor eigenstates, B_{flav}.

The total likelihood function for all categories is given as the product of the likelihoods over the seven tagging categories (including a category for untagged events for yield determination).

5 Results

The reconstruction efficiency is 10.3% and 11.6% for $\eta'_{\rho\gamma}K^0_L$ and $\eta'_{\eta\pi\pi}K^0_L$ respectively. In Table 1 we give the number of the signal yield and the parameters S and C. Note that the sign of the *CP* eigenvalue of the final state is out of the definition of S parameter (see Eqn. (1)), so S parameter has the same sign in $\eta' K^0_S$ and $\eta' K^0_L$ events. The $\eta' K^0_S$ data are those used in *BABAR* previous measurement [11]. Combining $\eta'_{\eta\pi\pi}K^0_L$ events and $\eta'_{\rho\gamma}K^0_L$ events, we measure $S = 0.60 \pm 0.31$ and $C = 0.10 \pm 0.21$. In this fit we have 42 free parameters: S, C, signal yields (2), $B\overline{B}$ background yield (1), continuum background yields (2) and fractions (12), background Δt, ΔE, $\mathcal{F}$, η' mass and $\mathcal{H}$ PDF parameters (23). In the final fit, combining $\eta' K^0_S$ and $\eta' K^0_L$, we have 138 free parameters: S, C, signal yields (7), $B\overline{B}$ background yield (3), continuum background yields (7) and fractions (42), background Δt, ΔE, $\mathcal{F}$, η' mass and $\mathcal{H}$ PDF parameters (77).

Table 1: Results with statistical errors for the $B^0 \to \eta' K^0$ time-dependent fits (decays with K^0_L in upper part on the table and decays with K^0_S in lower part of the table).

Mode	Signal yield	S	C
$\eta'_{\eta\pi\pi}K^0_L$	137 ± 22	0.38 ± 0.44	0.34 ± 0.29
$\eta'_{\rho\gamma}K^0_L$	303 ± 49	0.88 ± 0.43	-0.15 ± 0.29
$\eta'_{\eta(\gamma\gamma)\pi\pi}K^0_{\pi^+\pi^-}$	188 ± 15	0.01 ± 0.28	-0.18 ± 0.18
$\eta'_{\rho\gamma}K^0_{\pi^+\pi^-}$	430 ± 26	0.44 ± 0.19	-0.30 ± 0.13
$\eta'_{\eta(3\pi)\pi\pi}K^0_{\pi^+\pi^-}$	54 ± 8	0.79 ± 0.47	0.11 ± 0.35
$\eta'_{\eta(\gamma\gamma)\pi\pi}K^0_{\pi^0\pi^0}$	44 ± 9	-0.04 ± 0.57	-0.65 ± 0.42
$\eta'_{\rho\gamma}K^0_{\pi^0\pi^0}$	89 ± 23	-0.45 ± 0.68	0.41 ± 0.40
Combined fit	1245 ± 67	0.36 ± 0.13	-0.16 ± 0.09

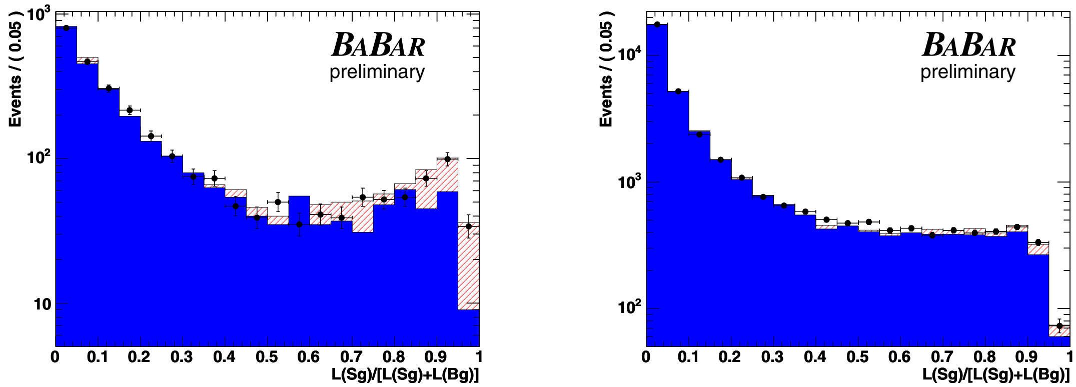

Figure 2: The likelihood ratio $\mathcal{L}(Sg)/[\mathcal{L}(Sg)+\mathcal{L}(Bg)]$ for $\eta'_{\eta\pi\pi}K^0_L$ (left) and $\eta'_{\rho\gamma}K^0_L$ (right). The points represent the on-resonance data, the histograms are from PDF generated events of background (blue area) and background plus signal (shaded red area).

The agreement between PDF simulated events and data is investigated using likelihood ratios. We generate signal and background Monte Carlo samples from the PDFs and, using the fitted parameter values from nominal fit, we calculate the likelihoods for both samples. In Fig. 2 we show the likelihood ratio $\mathcal{L}(Sg)/[\mathcal{L}(Sg)+\mathcal{L}(Bg)]$ for the two sub-decays $\eta'_{\rho\gamma}K^0_L$ and $\eta'_{\eta\pi\pi}K^0_L$ for data and for the PDF generated events. In Fig. 3 we show the projection onto ΔE of a subset of the data for which the signal likelihood (computed without the plotted variable) exceeds a mode-dependent threshold that optimizes the sensitivity. We show in Fig. 4 the Δt projection and asymmetry for $B^0 \to \eta' K^0_L$.

6 Systematic Uncertainties and Cross-checks

The contributions to the systematic uncertainties in S and C for $\eta' K^0_L$ are summarized in Table 2.

We evaluate the uncertainties associated with the PDF shapes by variation of the parameters describing each discriminating variable. Systematic errors associated with signal parameters (Δt resolution function, tagging fractions, and dilutions) are determined by varying their values within their errors. Uncertainties due to Δm_d and τ_B are obtained by varying these parameters by the uncertainty in their world average values [15]. All changes are combined in quadrature obtaining an error of 0.02 for S and 0.01 for C.

We vary the SVT alignment parameters in the signal Monte Carlo events by the size of misalignments found in the real data, and assign the resulting shift in the fit results as the systematic error of 0.01 for both S and C.

The systematic errors due to interference between the CKM-suppressed $\bar{b} \to \bar{u}c\bar{d}$ amplitude and the favored $b \to c\bar{u}d$ for some tag-side B decays are found to be negligible for S and gives a contribution to the C uncertainty of about 0.01.

The systematic error due to $B\overline{B}$ background is estimated to be 0.03 in S and 0.01 in C

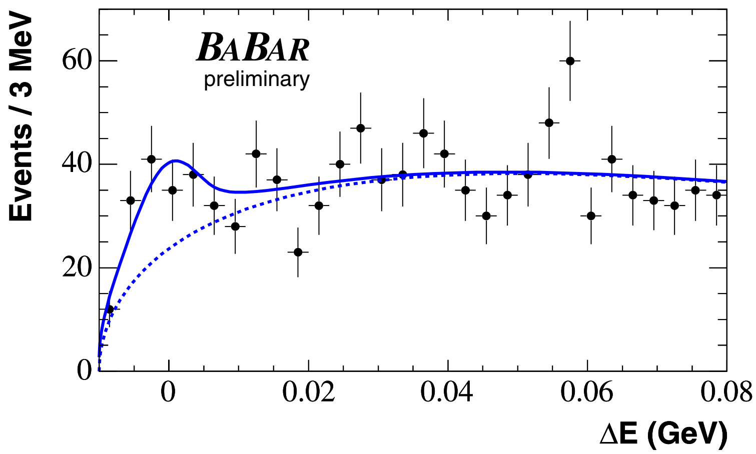

Figure 3: Projection onto ΔE for $B^0 \rightarrow \eta' K^0_L$ (sum of the sub-decay modes $\eta'_{\rho\gamma} K^0_L$ and $\eta'_{\eta\pi\pi} K^0_L$) of a subset of the data for which the signal likelihood (computed without the plotted variable) exceeds a mode-dependent threshold that optimizes the sensitivity. Points with errors represent the data, solid curve the full fit functions and dashed blue curve the total background functions.

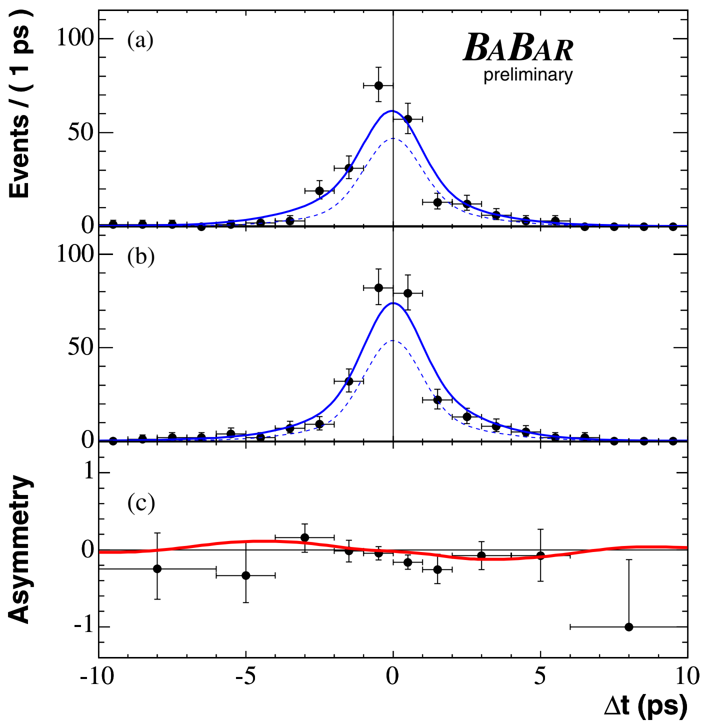

Figure 4: Projections onto Δt for $\eta' K^0_L$ (sum of the sub-decay modes $\eta'_{\rho\gamma} K^0_L$ and $\eta'_{\eta\pi\pi} K^0_L$) of a subset of the data for which the signal likelihood exceeds a mode-dependent threshold that optimizes the sensitivity. Points with errors represent the data, solide curve the full fit functions, and dashed blue curve the total background functions, for (a) B^0 and (b) $\overline{B}^0$ tagged events. The asymmetry between B^0 and $\overline{B}^0$ tags is shown in (c).

parameter. An uncertainty of 0.01 is assigned to account for limitations of Monte Carlo statistics and modeling of the signal. We assign an uncertainty of 0.01 to account for the uncertainty in the position and size of the beam spot, determined from variation of these quantities in signal MC. The total systematic error is obtained by summing individual errors in quadrature.

Table 2: Estimates of systematic errors for $\eta' K^0_L$.

Source of error	$\sigma(S)$	$\sigma(C)$
PDF Shapes	0.02	0.01
SVT alignment	0.01	0.01
Tag-side interference	0.00	0.01
$B\overline{B}$ Background	0.03	0.01
MC statistics/modeling	0.01	0.01
Beam spot	0.01	0.01
Total	0.04	0.03

We have also performed a number of checks of our results. When we fit the combined sample $\eta' K^0_S$ and $\eta' K^0_L$ with the value for C fixed to zero, we find $S = 0.37 \pm 0.13$. We produce samples of pseudo-experiments generated with events produced to match the PDF distributions. From these samples, we verify that the fit bias on S and C is negligible and that there is a good agreement between expected and observed errors. The fit was also verified with our $B^0 \to J/\psi K^0_L$ data sample.

7 Conclusion

In a sample of 232 million $B\overline{B}$ pairs we have reconstructed 137 ± 22 $\eta'_{\eta\pi\pi} K^0_L$ events and 303 ± 49 $\eta'_{\rho\gamma} K^0_L$ events. We use these events to measure the time-dependent asymmetry parameters S and C:

$$\begin{aligned} S &= 0.60 \pm 0.31 \ (\text{stat}) \pm 0.04 \ (\text{syst}) \\ C &= 0.10 \pm 0.21 \ (\text{stat}) \pm 0.03 \ (\text{syst}) \end{aligned}$$

Using this sample and the $\eta' K^0_S$ sample found in Ref. [11], we obtain a total of 1245 ± 67 $\eta' K^0$ events and with a combined fit of all data we measure:

$$\begin{aligned} S &= 0.36 \pm 0.13 \ (\text{stat}) \pm 0.03 \ (\text{syst}) \\ C &= -0.16 \pm 0.09 \ (\text{stat}) \pm 0.02 \ (\text{syst}) \end{aligned}$$

All these results are preliminary. Our result for S differs from the *BABAR* value of $\sin 2\beta = 0.722 \pm 0.040 \pm 0.023$ in charmonium decays [16] by 2.8 standard deviation.

8 Acknowledgments

We are grateful for the extraordinary contributions of our PEP-II colleagues in achieving the excellent luminosity and machine conditions that have made this work possible. The success of this project also relies critically on the expertise and dedication of the computing organizations that support *BABAR*. The collaborating institutions wish to thank SLAC for its support and the kind hospitality extended to them. This work is supported by the US Department of Energy and

National Science Foundation, the Natural Sciences and Engineering Research Council (Canada), Institute of High Energy Physics (China), the Commissariat à l'Energie Atomique and Institut National de Physique Nucléaire et de Physique des Particules (France), the Bundesministerium für Bildung und Forschung and Deutsche Forschungsgemeinschaft (Germany), the Istituto Nazionale di Fisica Nucleare (Italy), the Foundation for Fundamental Research on Matter (The Netherlands), the Research Council of Norway, the Ministry of Science and Technology of the Russian Federation, and the Particle Physics and Astronomy Research Council (United Kingdom). Individuals have received support from CONACyT (Mexico), the A. P. Sloan Foundation, the Research Corporation, and the Alexander von Humboldt Foundation.

References

[1] Y. Grossman and M. P. Worah, Phys. Lett. B **395**, 241 (1997)

[2] D. Atwood and A. Soni, Phys. Lett. B **405**, 150 (1997)

[3] D. London and A. Soni, Phys. Lett. B **407**, 61 (1997).

[4] M. Beneke and M. Neubert, Nucl. Phys. B **651**, 225 (2003).

[5] Y. Grossman *et al.*, Phys. Rev. D **68**, 015004 (2003).

[6] C.-W. Chiang, M. Gronau and J. L. Rosner, Phys. Rev. D **68**, 074012 (2003).

[7] M. Gronau, J. L. Rosner and J. Zupan, Phys. Lett. B **596**, 107 (2004); M. Gronau, Nucl. Phys. Proc. Suppl. **142**, 263-270 (2005).

[8] *BABAR* Collaboration, B. Aubert *et al.*, Phys. Rev. Lett. **93**, 181806 (2004)

[9] *BABAR* Collaboration, B. Aubert *et al.*, Phys. Rev. D **70**, 032006 (2004)

[10] M. Beneke and M. Neubert, Nucl. Phys. B **675**, 333 (2003).

[11] *BABAR* Collaboration, B. Aubert *et al.*, Phys. Rev. Lett. **94**, 191802 (2005).

[12] Belle Collaboration, K. Abe *et al.*, Phys. Rev. Lett. **91**, 261602 (2003).

[13] *BABAR* Collaboration, B. Aubert *et al.*, Nucl. Instr. Meth. A **479**, 1 (2002).

[14] PEP-II Conceptual Design Report, SLAC-R-418 (1993).

[15] Particle Data Group, S. Eidelman *et al.*, Phys. Lett. B **592**, 1 (2004).

[16] *BABAR* Collaboration, B. Aubert *et al.*, Phys. Rev. Lett. **94**, 161803 (2005).